THE TODOROKITE FROM KARSTIC MANGANIFEROUS CONCENTRATIONS OF KALAMATA AREA (PELOPONNESE, GREECE)

A. PHOTIADES[1], E. A. PERSEIL[2] & R. GIOVANOLI[3]

[1]*Institute of Geology & Mineral Exploration, Athens, Greece*
[2]*Museum National Histoire Naturelle, Paris, France*
[3]*University of Berne, Switzerland*

Abstract: The Mn-mineralisation of Kalamata area occurs in karstic cavities within the Eocene to Upper Cretaceous limestone of the Tripolis isopic zone (External Hellenides), and is overlain by Plio-Quaternary sediments.

The morphological and mineralogical features of todorokite reveal that it developed at the expense of pyrolusite under reducing conditions during its precipitation from the manganese-bearing solutions.

Key words: Todorokite, SEM, X-ray, IR spectrum, Peloponnese, Greece.

The manganese occurrences of Kalamata (Leika district) have been exploited from 1927 to 1956. The composition of the ore was Mn 38-40% and $Si0_2$ 7-9%, with a total production of 40.000 tons (Liatsikas et al. 1947; Mousoulos 1962). The manganiferous mineralisation has been attributed to a sedimentary origin, related to karstification processes (Putzer 1948; Kiskyras 1957; Mousoulos 1962; Gruszczyk et al. 1970).

The Eocene to Upper Cretaceous limestone is overlain by Eocene-Oligocene flysch deposits (Fig. 1), which both belong to the Tripolis isopic zone of the External Hellenides (Thiebault 1982; Psonis et al. 1986). It is noted that locally there are Pindos zone klippes, comprising manganiferous red cherts associated with thin-bedded limestone overthrust on the previous flysch. Post-Miocene NW-SE trending faults (Mariolakos et al. 1985) probably contributed to the karstification process, and the collapse of the overlying flysch, which presently occurs as breccia in the karstic cavities. Subsequently, the Mn-mineralisation was probably deposited in pre-existing karstic cavities during the Lower Pliocene tectonic movements affecting the area, which have influenced the whole Plio-Quaternary sequence. The deeper parts of the Plio-Quaternary cover deposits are cemented by carbonates and locally by manganese oxides.

This paper re-examines the mineralogy of Leika district, and especially the mineralogical features of todorokite using various techniques of investigation.

Microscopic examination under reflected light on these manganese oxides revealed that pyrolusite and todorokite are both important and comparable in all mineralogical examinations. Pyrolusite appears in fine-crystallised (Fig. 2a) or coarse-crystallised aggregates (Fig. 2b). Whereas, todorokite occurs in large concretions developed inside pyrolusite plates (Fig. 2a and b); additionally, the pyrolusite appears as residual islets within todorokite concretions.

It is confirmed by scanning electron microscope (SEM) that the crystallised pyrolusite aggregates are progressively replaced by the characteristically needle-shaped todorokite (Fig. 2c and d). In all microscopic observations, under different scales, it has been observed that todorokite is always formed at the expense of pyrolusite.

X-ray diffraction patterns of todorokite (Fig. 3) confirm that the values of interplanar d-spacing of the lattice planes of this mineral are very close to todorokite from Charco Redondo of Cuba (after Powder Diffraction File, JCPDS 18-1411), as well as to todorokite from Ambollas of Eastern Pyrenees, France (Perseil & Giovanoli, 1982); it is also noted on the X-ray films the occurrence of calcite and quartz rays (Table 1).

Besides, the infrared spectra of todorokite (Nicolet 740/I.R. Plane II) indicate a large diversity in the order of its crystalline structure, especially between 3200 cm^{-1} to 3400 cm^{-1} regions. For this reason, it can be noted that towards the 3200 cm^{-1} region (Fig. 4) the well-resolved band intensities (Fig. 4a and c) reveal more ordered todorokite structure than those, which indicate a larger band in the 3200 cm^{-1} to 3400 cm^{-1} region (Fig. 4b). According to Potter & Rossman (1979) the enlargement of the observed band is due to a disordered todorokite structure.

Microprobe analyses (Table 2, where each analysis represents the average of 30 analyses) reveal the low content in iron and transition elements, similar in chemistry to the Cuban todorokite (Frondel et al. 1960). Furthermore, the analysed todorokite is characterised by Ba, Sr, K and Na. The former two elements suggest that they are derived from the Eocene to Upper Cretaceous limestone.

The low content in iron favoured the formation of well-crystalised todorokite under pH conditions greater than 7, because in lower pH-values this mineral is unstable (Giovanoli et al. 1975; Halbach et al.1975). Further, the occurrence of pyrolusite before the todorokite crystallization indicates an oxidation stage during the precipitation of pyrolusite from the manganiferous solutions.

The origin of manganese may have been derived from the continuous leaching and weathering of manganiferous red chert klippes of the Pindos zone occurring in the vicinity of the study area.

References

Frondel C., Marvin U.B. & Ito J. (1960). New occurrences of todorokite. *Am. Mineral 45, 1167-1173*.

Giovanoli R., Burki P., Giuffredi M. and Stumm W. (1975). Layer structured manganese oxide hydroxides. IV-The buserite group; structure stabilization by transition elements. Chimia, Zurich, 29, 110-113.
Gruszczyk H., Haranczyk C. and Melidonis N. (1970). About the results of mineral exploration of Peloponnesus. *Geol. Res. 49. IGSR* Athens (in Greek language with German summary).
Halbach P., Ozkara M. & Hence J. (1975). The influence of metal content on the physical and mineralogical properties of pelagic manganese nodules. Mineral.Deposita, 10, 397-411.
Kiskyras D. (1957). The manganese deposits of Peloponnesus. *Peloponnisiaka, 2: 271-286* Athens (In Greek language).
Liatsikas N., Solomos I., Kogevinas S. & Andreakos G. (1947). The mineral wealth of Greece. *UNRRA* Athens 1947 (In Greek language).
Mariolakos I., Papanikolaou D. & Lagios E. (1985). Neotectonic geodynamic model of Peloponnesus based on morphotectonics, repeated gravity measurements and seismicity. *Geol. Jb., B50, 3-17.*
Mousoulos L. (1962). The exploitation problem of the underground wealth of Greece. *Academy of Athens 1962* (In Greek language).
Perseil E.A. and Giovanoli R. (1982). Etude comparative de la todorokite d'Ambollas (Pyrenees Orientales), des manganates a 10 Å rencontres dans les nodules polymetalliques des oceans et des produits de synthese. *C.R. Acad. Sc. Paris, 294, 199-202*.
Potter R.M. and Rossman G.R. (1979). The tetravalent manganese oxides: identification, hydration, and structural relationships by infrared spectroscopy. *Am. Mineral. 64, 1199-1218*.
Psonis C., Tsapralis V., Varti-Mataranga M. and Petridou V. (1986). Geological map of Greece «Kalamata sheet» in scale 1:50.000. Athens IGME, Greece.
Putzer H. (1948). Les gisements de manganese du Peloponnese. *Ann. geol. Pays Hellen. 2, 47-60*.
Thiebault F. (1982). Evolution geodynamique des Hellenides externes en Peloponnese meridional (Grece). *Soc. geol. Nord, Publication n°6, 574 pp. (Lille).*

Fig. 1. Geological position of Kalamata area in relation to tectono-stratigraphic isopic zones of southern Hellenides (**A**) and the geological map of the study area (**B**); Ionian zone (IOZ); Plattenkalk zone (PLT); Gavrovo-Tripolis zone (GTZ); Pindos zone (PIZ); Subpelagonian zone (SPZ); Quaternary deposits (**1**); Plio-Plistocene deposits locally with Mn-occurrences (**2** & **3**); Jurassic-Lower Cretaceous Mn-rich bedded red chert and sandstone overlying by Upper Cretaceous bedded limestones of Pindos zone klippes (**4**); Eocene-Oligocene flysch of Tripolis zone (**5**); Eocene limestone (**6**); Upper Cretaceous to Middle Triassic limestone and dolomitic limestone (**7**); Permian-Lower Triassic Tyros beds (**8**); Autochthonous series of Plattenkalk zone (**9**); fault (**f**); thrust (**t**); strike and dip of beds (**d**); Mn-mineralisation of Leika district (**Mn**).

Fig. 2. Pyrolusite (**p**) as fine-crystallised (**a**) or coarse-crystallised aggregates (**b**) and todorokite (**t**) as large concretions (Reflected light, scale bar is 20μm). SEM micrographs revealing the well-crystallized pyrolusite (**c**), which is replaced by needle-shaped todorokite (**d**).

Fig. 3. X-ray diffraction patterns of torokite from Kalamata (Greece) and Ambollas (France) [with • (=β-$Mn0_2$, pyrolusite), **χ** (=α-$Si0_2$), **o** (=$CaCO_3$, calcite)].

Fig. 4. IR spectra of todorokite with ordered (**a, c**) and disordered structures (**b**).

Table 1. X-ray powder diffraction data of todorokite from Kalamata compared to those of Ambollas (France) and Charco Redondo (Cuba).

Table 2. EMP analyses of todorokite from Kalamata.

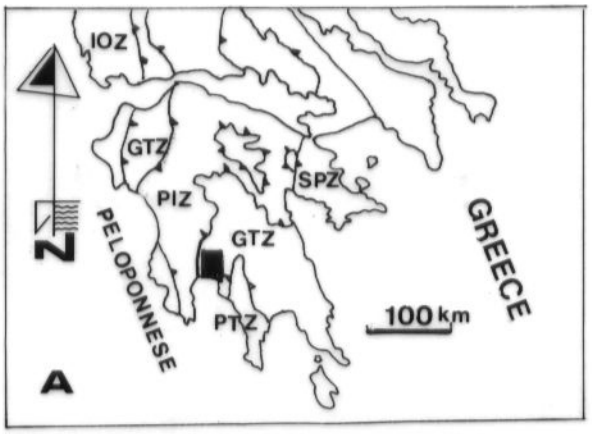
IOZ
GTZ
PIZ
SPZ
GTZ
PTZ
PELOPONNESE
GREECE
100 km
N
A

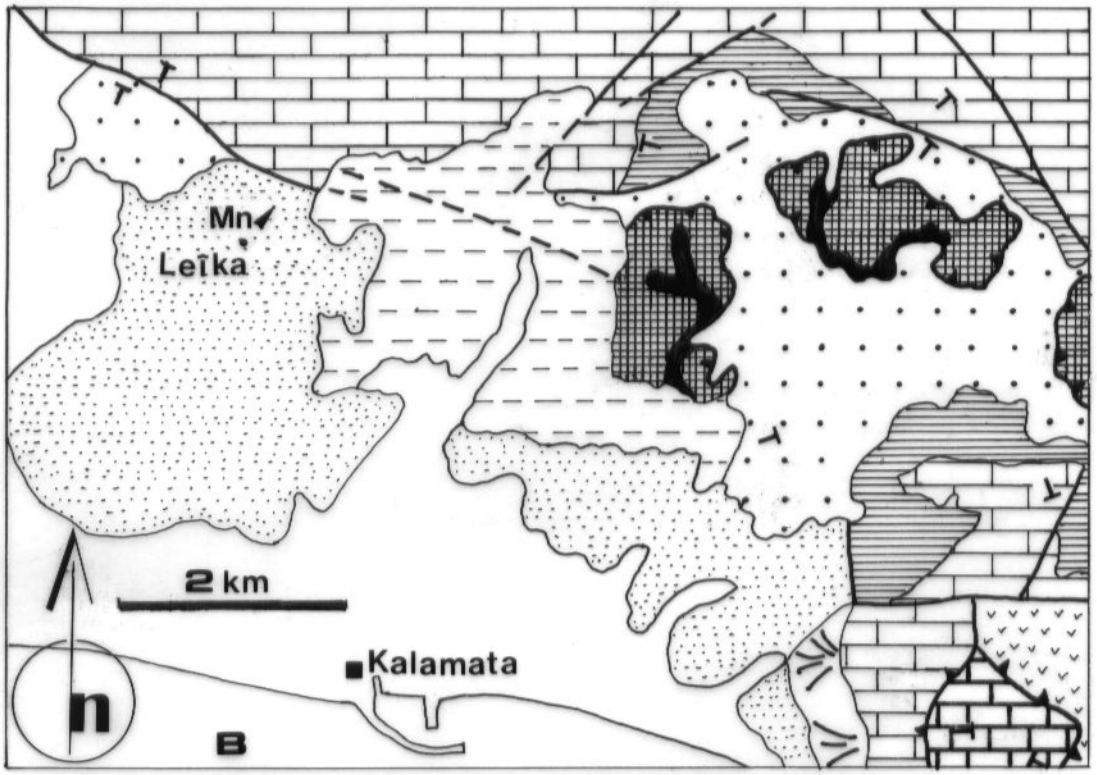
Mn
Leïka
2 km
Kalamata
n
B

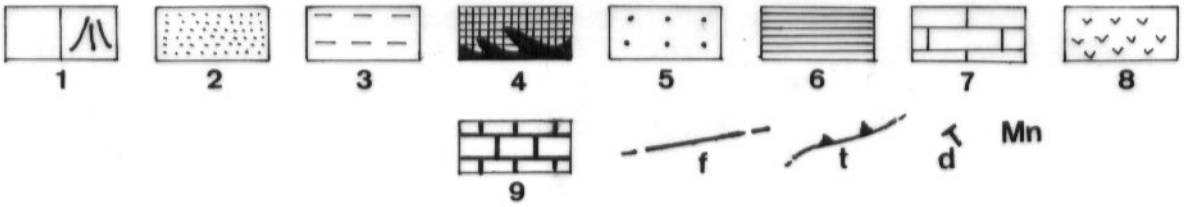
1
2
3
4
5
6
7
8
9
f
t
d
Mn

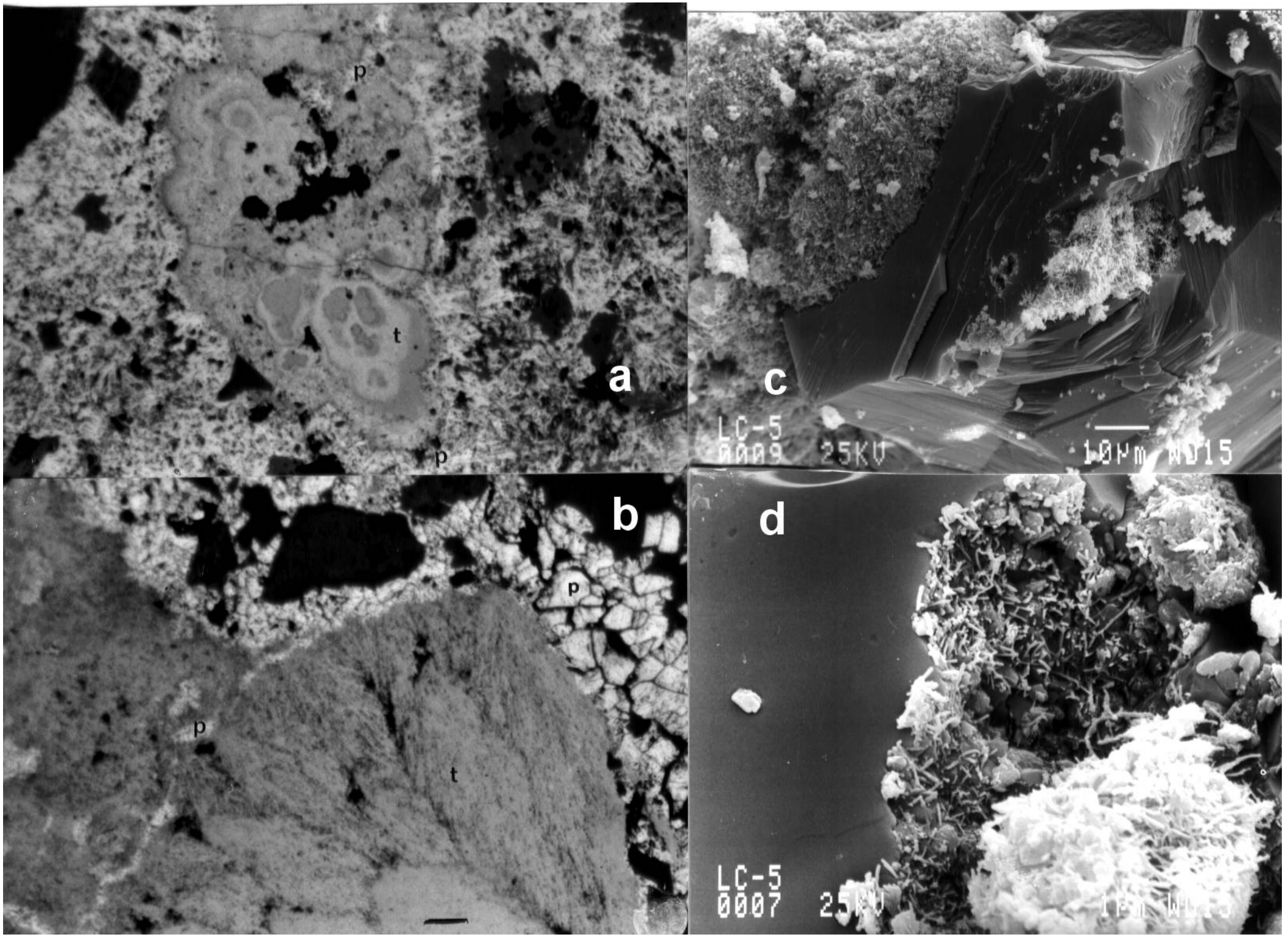
p
t
a
p
c
LC-5
0009 25KV
10µm WD15
b
p
p
t
d
LC-5
0007 25KV

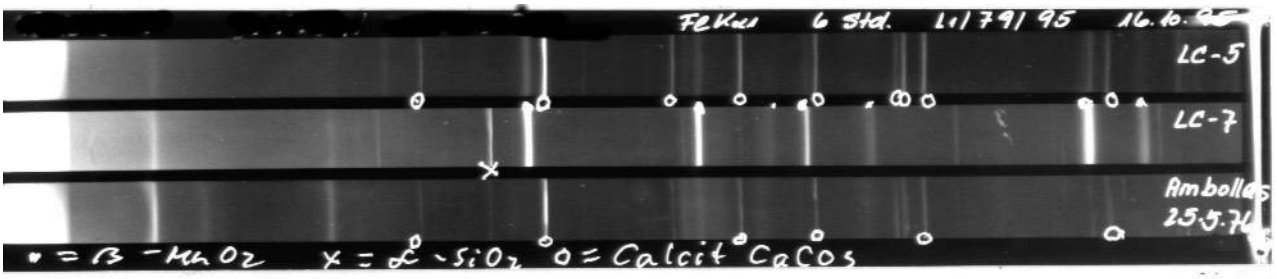
LC-5
LC-7
Amboll
25.5.7
• = β -Mn O2 x = α -Si O2 ° = Calcit Ca CO3

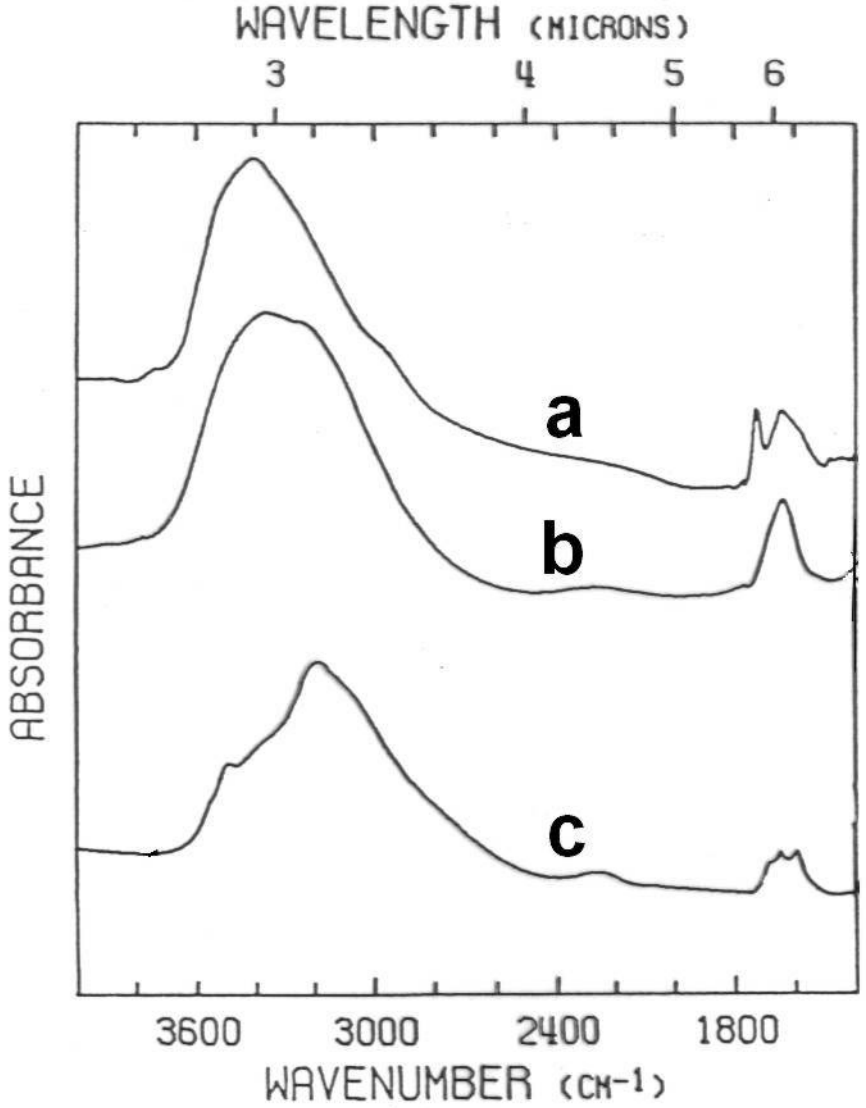
WAVELENGTH (MICRONS)
3
4
5
6
a
b
c
ABSORBANCE
3600
3000
2400
1800
WAVENUMBER (CM-1)

Table 1

Kalamata (Greece)		Ambollas (Eastern Pyrenees France)		Charco Redondo (Cuba) JCPDS 18-1411	
d(A)obs	I obs	d(A)obs	I obs	d(A)obs	I obs
9.68	100	9.69		9.65	80
7.14	5	7.53		7.02	40
4.81	80	4.82		4.82	70
4.43	10	2.40		4.48	70
3.33	50qz	2.36		3.20	10
3.03	50cc			3.07	40
2.48	10cc			2.75	10
2.42	20			2.46	40
2.39	20cc			2.42	10
2.27	10cc			2.35	40
1.97	5			2.28	10
				2.20	5
	qz:quartz line			2.13	10
	cc:calcite line			1.98	10
				1.91	5
				1.77	10
				1.67	10
				1.64	10
				1.54	10
				1.42	5
				1 406	5

	1	2	3	4	5	6	7	8
MnO2	68.31	69.57	73.02	74.07	75.25	75.36	75.39	75.48
Fe2O3	0.52	1.07	0.33	0.17	0.20	0.12	0.01	0.00
Al2O3	4.23	1.84	1.81	0.93	0.74	0.60	0.76	0.76
NiO	0.17	0.13	0.00	0.00	0.06	0.14	0.00	0.06
CoO	0.00	0.14	0.09	0.08	0.00	0.00	0.00	0.00
CaO	1.39	1.60	1.37	1.64	1.29	1.32	1.56	1.49
BaO	3.17	4.98	2.04	2.59	1.87	2.05	3.26	2.86
MgO	5.22	3.05	3.45	3.37	3.04	2.97	3.00	2.99
K2O	0.61	0.81	0.82	0.81	1.61	1.30	0.95	0.95
Na2O	0.43	0.38	0.48	0.72	0.58	0.69	0.69	0.81
SiO2	2.22	2.72	4.23	2.97	1.59	2.59	2.27	2.63
SrO	0.29	0.36	0.02	0.08	0.41	0.41	0.04	0.00
?	86.56	86.83	87.66	87.43	86.64	87.55	87.93	88.03
H2O	11.84	11.56	12.13	11.91	11.71	11.89	11.88	11.93